Antiviral Research 96 (2012) 363–375

Contents lists available at SciVerse ScienceDirect

Antiviral Research

journal homepage: www.elsevier.com/locate/antiviral

Prophylactic, therapeutic and neutralizing effects of zinc oxide tetrapod structures against herpes simplex virus type-2 infection

Thessicar E. Antoine [a,b], Yogendra K. Mishra [c], James Trigilio [a], Vaibhav Tiwari [a,d], Rainer Adelung [c], Deepak Shukla [a,b,*]

[a] Department of Ophthalmology & Visual Sciences, University of Illinois at Chicago, IL 60612, USA
[b] Department of Microbiology & Immunology, University of Illinois at Chicago, IL 60612, USA
[c] Institute for Materials Science, University of Kiel, Kiel 24143, Germany
[d] Department of Microbiology–Immunology, Midwestern University, Downers Grove, IL 60515, USA

ARTICLE INFO

Article history:
Received 17 August 2012
Revised 25 September 2012
Accepted 27 September 2012
Available online 6 October 2012

Keywords:
Herpes
Heparan sulfate
Zinc oxide
Herpes simplex virus
Entry
Glycoproteins

ABSTRACT

The attachment of Herpes simplex virus type-2 (HSV-2) to a target cell requires ionic interactions between negatively charged cell surface co-receptor heparan sulfate (HS) and positively charged residues on viral envelop glycoproteins, gB and gC. Effective blocking of this first step of HSV-2 pathogenesis demonstrates significant prophylactic effects against the viral disease; any in vitro therapeutic effects of blocking this interaction, however, are not clear. Here, we provide new evidence that zinc oxide tetrapod micro-nanostructures synthesized by flame transport approach significantly block HSV-2 entry into target cells and, in addition, demonstrate the potential to stop the spread of the virus among already infected cells. The zinc oxide tetrapods (ZnOTs) also exhibit the ability to neutralize HSV-2 virions. Natural target cells such as human vaginal epithelial and HeLa cells showed highly reduced infectivity when infected with HSV-2 virions that were pre-incubated with the ZnOTs. The mechanism behind the ability of ZnOTs to prevent, neutralize or reduce HSV-2 infection relies on their ability to bind the HSV-2 virions. We used fluorescently labeled ZnOTs and GFP-expressing HSV-2 virions to demonstrate the binding of the ZnOTs with HSV-2. We also show that the binding and hence, the antiviral effects of ZnOTs can be enhanced by illuminating the ZnOTs with UV light. Our results provide new insights into the anti-HSV-2 effects of ZnOT and rationalize their development as a HSV-2 trapping agent for the prevention and/or treatment of infection. The observed results also demonstrate that blocking HSV-2 attachment can have prophylactic as well as therapeutic applications.

1. Introduction

HSV-2 is one of the most frequent sexually transmitted infections worldwide with global estimates of 536 million infected people and an annual incidence of 23.6 million cases (Tronstein et al., 2011). In the United States alone, 22% adults are HSV-2 seropositive (Wald et al., 2001), but only a small percentage of individuals with HSV-2 infections have been recognized with genital herpes. Additionally, most HSV-2 infections are acquired from persons without a clinical history of genital herpes, thus the risk of sexual transmission does not correlate well with the recognition of clinical signs and symptoms of HSV-2 (Shukla et al., 2009). HSV-2 infection results in a wide variety of clinical manifestations ranging from asymptomatic infections to ulcerative and vesicular lesions on the genitals. The latter is a hallmark site of infection. The infection, however is not limited to the genital area, as it is capable of causing necrotizing stromal keratitis in the eye, encephalitis, meningitis and neurological complications in infants surviving the infection (Chayavichitsilp et al., 2009; Jin et al., 2011; Kriebs, 2008). HSV-2 infections are rarely fatal but the presence of herpetic lesions on the mother during the birth process places babies' lives at risk (Spear, 2004). Despite its vast presence in the population, no cure or vaccination has been developed causing people to live with either symptomatic and/or asymptomatic recurrences for the rest of their lives.

HSV-2 is the prototype of the neurotropic alphaherpesviruses, all of which cause latency (Avitabile et al., 2007). The virion consists of an electron dense core containing double stranded DNA that encodes over seventy different genes. The genome of the virus is enclosed by an icosahedral capsid that displays 162 protein units known as capsomers (Akhtar and Shukla, 2009; Favoreel et al., 2010; Jackson and Longnecker, 2010). The capsid, in turn, is surrounded by tegument proteins and all components are enclosed

* Corresponding author at: Department of Ophthalmology & Visual Sciences, University of Illinois at Chicago, IL 60612, USA. Tel.: +1 312 355 0908; fax: +1 312 996 7773.
E-mail address: dshukla@uic.edu (D. Shukla).

0166-3542/$ - see front matter © 2012 Elsevier B.V. All rights reserved.
http://dx.doi.org/10.1016/j.antiviral.2012.09.020

by a lipid bilayer envelope with over a dozen viral proteins and glycoproteins on the surface (Campadelli-Fiume et al., 2000). Of the many glycoproteins on the envelope, five are important for the coordination of host cell entry: gB, gC, gD, gH, and gL (Connolly et al., 2011). While gB and gC facilitate HSV attachment to cells by binding with negatively charged heparan sulfate (HS), others including gB are required for the capsid penetration into the host cells. Blocking attachment of the virus is known to have prophylactic effects against the disease; however, it is not clear whether blocking attachment can generate therapeutic effects against existing infections as well. The ability of HSV to typically infect any cell type makes the development of more efficient therapeutics a high priority. In addition, the lifelong prevalence of HSV-2 infection results in prolonged administration of standard treatments leading to an increased risk of drug resistance against existing HSV antivirals, which mostly target HSV replication (Muggeridge, 2000). Thus, new drugs that target other critical steps in viral lifecycle such as entry and cell-to-cell spread can help reduce the risk of the emergence of drug resistance.

Recent exploration of nanoparticle interactions with biological targets has transformed the field of medical research including the area of drug development (Wiesenthal et al., 2011). In this regard the recently described ZnO micro-nano particles have shown high promise as prophylactic agents against HSV-1 (Mishra et al., 2011). In the present work we have examined the anti-HSV-2 properties of ZnO tetrapod (ZnOT) structures synthesized by the flame transport approach (Adelung et al., 2011). We describe the neutralizing, prophylactic, and therapeutic applications of ZnOTs against HSV-2 infection in vitro and establish a mechanism by which ZnOT bind HSV-2 virions and render them ineffective for a productive infection.

2. Materials and methods

2.1. Synthesis of ZnO tetrapod structures and cytotoxicity assay on cells

ZnOT structures were synthesized by a recently developed flame transport synthesis (FTS) approach (Adelung et al., 2011). Briefly, the Zn metal micro powder (commercially available from Goodfellows, UK) was mixed with sacrificial polymer powder (Polyvinyl Butyrol, Kuraray GmbH Europe) and the mixture was then burned at 900 °C in a simple muffle type box furnace in air which resulted in the formation of ZnOTs (Adelung et al., 2011; Mecklenurg et al. (2012)). The tetrapods were then harvested from the furnace and used for the antiviral tests. The shape and size of the synthesized structures were investigated using scanning electron microscopy (SEM) at 10 kV electron beam acceleration voltage and 18 μA filament (LaB_6) current. The SEM results confirmed the tetrapod shape of the ZnO structures with arm diameters in the range of 200 nm to 1 μm and arm lengths in the range of 5–30 μm. Identical ZnOTs were used for all experiments demonstrated here.

To determine the effect of UV ZnOT and NUV ZnOT treatment on the viability of HeLa and VK2/E6 cells an MTS cytotoxicity assay was performed 24 h after ZnOT treatment. V2 K/E6 cells and HeLa cells were seeded at a density of 2×10^4 in a 96-well plate. UV treated ZnOT was spread in a thin layer and placed in a petri dish for irradiation for 1 h. UV ZnOT and NUV ZnOT were brought into suspension in PBS at concentrations of 1.5, 1, 0.8, 0.6, 0.4, 0.2, and 0.1 mg/mL. Removal of culture medium from confluent monolayer of cells was followed by treatment with the various concentrations of UV and NUV ZnOT for 24 h. Cell viability was analyzed by a chromogenic kit (CellTiter Aqueous96; Promega, Madison, WI, USA). Colorimetric detection was measured by micro-pate reader (TECAN GENious Pro) at 492 nm.

2.2. Cells, virus, plasmids and antibodies

Chinese hamster ovary (CHO-K1) cells were provided by P.G. Spear (Northwestern University). CHO-K1 cells were passaged in Ham's F12 medium (Gibco/BRL, Carlsbad, CA, USA) supplemented with 10% fetal bovine serum (FBS) and penicillin and streptomycin (P/S) (Sigma). HeLa cells were provided by B.P. Prabhakar (University of Illinois Chicago) which were passaged in Dulbecco's modified Eagle's medium (DMEM) supplemented with 10% FBS and P/S. African green monkey kidney (Vero) cells were provided by P.G. Spear (Northwestern University). Vero cells were passaged in Dulbecco's modified Eagle's medium (DMEM) supplemented with 10% FBS and P/S. Human vaginal epithelial (VK2/E6) cells were obtained from ATCC. VK2/E6 cells were passaged in Karatinocyte serum free medium (SFM) (Gibco/BRL, Carlsbad, CA, USA) supplemented with epidermal growth factor (EGF) and bovine pituitary extract (BPE).

Wild type HSV-2(333), HSV-2(333) GFP, and β-galactosidase-expressing HSV-2(333)gJ− were also used (Martinez and Spear, 2002). Virus stocks were propagated and tittered on Vero cells, and stored at −80 °C.

The plasmids expressing HSV-2 glycoproteins pMM245 (gB), pMM346 (gD), pMM349 (gH) and pMM350 (gL) were used in this study (Muggeridge, 2000; O'Donnell and Shukla, 2009). Plasmid pT7EMCLuc that expresses firefly luciferase gene under the control of a T7 promoter and plasmid pCAGT7 that expresses T7 RNA were also used (Pertel et al., 2001; Tiwari et al., 2004).

The following primary antibodies were used for Western blot analysis in this study: Mouse anti-VP16 monoclonal antibody (mAB) diluted 1:500 (sc-7545 Santa Cruz Biotechnology, Santa Cruz, CA); rabbit anti-GAPDH at 1:2000 polyclonal antibody diluted 1:2000 (sc-25778 Santa Cruz Biotechnology, Santa Cruz, CA). Secondary antibodies used for western blot analysis were horseradish peroxidase-conjugated anti-mouse IgG diluted1:25000 (115–035-062, Jackson ImmunoResearch Laboratories) and horseradish peroxidase-conjugated goat anti-rabbit IgG diluted 1:20000.

2.3. ZnOT treatment conditions

2.3.1. Neutralization treatment

To determine the neutralizing properties of ZnOTs, HSV-2(333), HSV-2(333)gJ−, and HSV-2(333)GFP virus underwent "turn-cubation", a method we recently designed to optimize the binding between ZnOT and HSV-2. Turn-cubation is the process in which HSV-2 virus and ZnOT (UV: ultra violet treated, NUV: Non-UV treated) undergo a constant 360 rotation (260250 Orbitron Rotator II) for 1 h at 4 °C. At a concentration of 0.1 mg/ml ZnOT were incubated with virus at an MOI of 1 or 0.1. At the completion of the incubation step the suspension containing the virus and ZnOTs is added to the HeLa cells and V2 K/E6 cells. β-Galactosidase expression, VP16 detection, plaque formation, infectious viral cluster number and size measurements were performed thereafter. 1× PBS mock treated samples were used as a positive control to determine HSV-2 infectivity in the absence of ZnOTs.

2.3.2. Prophylactic treatment

To determine the efficacy of ZnOT as a prophylaxis against HSV-2, the cells were pretreated with 0.1 mg/ml of UV or NUV ZnOT for 30 min at 37 °C in the absence of the virus. At the end of the 30 min incubation, cells were infected with an MOI of 1 or 0.1 and then placed at 37 °C from 2–6 h. At the end of the infection cells were washed with 1× PBS. β-Galactosidase expression, VP16 detection, plaque formation assay, and infectious viral cluster number and size measurements were performed to determine the effectiveness of the prophylaxis treatment on HSV-2 infection.

2.3.3. Therapeutic treatment

The therapeutic usage of ZnOTs was determined by first challenging the cells with HSV-2 at a MOI of 1 or 0.1 for 30 min at 37 °C in the absence of ZnOTs. Following the first 30 min of infection, HeLa cells and Vaginal cells were treated with UV, NUV ZnOT or mock treated with 1× PBS. β-Galactosidase expression, VP16 detection, plaque formation number and size, and infectious viral cluster number and size measurements were performed to establish the effectiveness of the therapeutic treatment on HSV-2 infection.

2.4. Viral entry assay

A standard entry assay was performed as described previously (Shukla et al., 1999). Briefly, HeLa and VK2/E6 cells were seeded at a density of 2×10^4 in a 96-well plate. Entry was examined under neutralization, prophylaxis, therapeutic or mock treatment (1× PBS) conditions. A stock concentration of 0.1 mg/ml of UV and NUV ZnOT's was used for each treatment condition. For the infection step, the cells were infected at an MOI of 1 with β-galactosidase expressing recombinant virus HSV-2(333)gJ− for 6 h at 37 °C. After 6 h cells were washed with PBS and the soluble substrate *o*-nitrophenyl-β-D-galactopyranoside (ONPG) was added. Enzymatic activity was measured by micro-pate reader (TECAN GENious Pro) at 405 nm.

2.5. Immunoblotting

After 2 h of infection with HSV-2(333) strain at an MOI of 1, the effectiveness of neutralization, prophylaxis, and therapeutic treatment on viral internalization in HeLa cells was determined by Western blot analysis (Shukla et al., 2009). Briefly, virally infected cell lysates (mock treated or treated with a concentration of 0.1 mg/ml of UV or NUV ZnOTs) were denatured in NuPAGE LDS Sample Buffer (Invitrogen,NP00007) and heated to 80 °C for 10 min. Equal amounts of protein were added to 4–12% SDS–PAGE and transferred to a nitrocellulose membrane. Nitrocellulose membrane was blocked in 5% nonfat milk in tris buffer saline (TBS) for 2 h at room temperature. After the nonspecific binding blocking step was complete, membranes were incubated with mouse anti-VP16 monoclonal antibody (Santa Cruz) at dilutions of 1:500 overnight at 4 °C. The following day the blots were washed multiple times with 0.1% TTBS (0.1% Tween 20 in TBS) before the addition of horse radish peroxidase conjugated anti-mouse IgG at dilutions of 1:25000 at room temperature. Protein bands were visualized on an ImageQuant LAS 4000 imager (GE Healthcare Life Sciences) after the addition of SuperSignal West Femto maximum sensitivity substrate (Pierce, 34096). The density of the bands were quantified using ImageQuant TL image analysis software (version:7). GAPDH was measured as a loading control.

2.6. Plaque assay and infectious spread assay

2.6.1. Plaque assay

A monolayer of HeLa cells was seeded in a 24 well plate at a density of 5×10^4 cells per well. Upon confluency the cells either received neutralization, prophylaxis, therapeutic or mock treatment (1× PBS) and a low MOI of 0.1 infection with HSV-2(333). Stock concentration of 0.1 mg/ml was used in treatment condition. After 2 h of infection at 37 °C inoculums were removed and methylcellulose (Sigma) was added over each monolayer. Cells were then incubated at 37 °C for 72 h. At the end of the incubation cells were fixed with methanol for 20 min at room temperature and stained with crystal violet. Plaques were counted and imaged at 10× objective (Zeiss Axiovert 200).

2.6.2. Infectious spread assay

The virus spread assay was performed as described previously (Roller and Herold, 1997). Briefly, a monolayer of HeLa cells received neutralization, prophylaxis, therapeutic, or mock treatment (1× PBS). A stock concentration of 0.1 mg/ml of ZnOT was used to for treatment. HeLa cells and were challenged with HSV-2(333)GFP strain at a low MOI of 0.1. 2 h post infection inoculum was removed. Cells were washed once with PBS and overlaid with methylcellulose (Sigma) DMEM medium. 72 h post infection the spread of HSV-2(333)GFP amongst HeLa cells was assessed by capturing images of the green virally infected cells clusters at 10× objective (Zeiss Axiovert 200). Cluster sizes were determined by outlining the area of each cluster, for each outline an average area was generated by Axioversion software.

2.6.3. Plaque size determination

A monolayer of HeLa cells were seeded in a 24 well plate at a density of 5×10^4 . Upon confluency cells received neutralization, prophylaxis, therapeutic or mock treatment (1× PBS). A 0.1 mg/ml stock of ZnOT's was used for each treatment condition. Cells were infected at an MOI of 0.1 with HSV-2(333) or HSV-2(333) GFP. After 2 h of infection at 37 °C inoculums were removed and methylcellulose was added. Seventy two hours post infection plaques were measured with a micrometer at the 10× objective. The area of each plaque was calculated using Axioversion software. The average area was determined by measuring 20 plaques from each group.

2.7. Cell-to-cell fusion assay

A standard virus free cell-to-cell fusion assay was performed as described previously (Tiwari et al., 2004). Two populations of CHO-K1 cells, designated target cells and effector cells were generated. The target cell population was transfected with 1.0 μg of gD receptor (nectin-1) and 0.5 μg of the plasmid expressing the luciferase gene. The effector cell population was transfected with 0.5 μg each of HSV-2 glycoproteins gB, gD, gH, and gL and T7 RNA polymerase. Effector cells lacking gB were used as a negative control. 18 h post transfection effector cells were treated with 0.1 mg/ml of UV ZnOT, 0.1 mg/ml NUV ZnOT or mock treated with (1× PBS). To determine fusion target and effector cells were mixed together (1:1 ratio) and co-cultured in 24 well dishes. 24 h post mixing effector and target cells luciferase gene expression resulting from fusion was measured using a reporter lysis assay (Promega).

2.8. Fluorescently labeled ZnOT binding to HSV(333) GFP virus

The binding ability of ZnOT to HSV-2(333) GFP was determined by mixing fluorescently labeled ZnOT with HSV-2(333)GFP. A thin layer of ZnOT powder was spread onto a petri dish. The ZnOT were illuminated with UV light for 1 h at room temperature. Five milligrams UV treated (UV) and five milligrams untreated (NUV) ZnOT were put into individual solutions (5 mg/ml). 1 ml of UV and NUV solutions were placed into Eppendorf tubes. Rhodamine phallodin (Legarra et al., 2008) (Invitrogen) was incubated at room temperature with ZnOTs for 20 min. At the end of incubation these ZnOT structures were washed twice with 1× PBS. HSV-2(333) GFP and fluorescently labeled ZnOTs were then placed into a 35 mm glass-bottom dish and incubated for 2 h at 37 °C(MatTek Corporation). At the end of incubation fluorescently label ZnOTs and HSV(333)GFP were imaged using a confocal microscope (Lecia DMIRE2) equipped with a camera (Lecia TCSSP2).

2.9. Syncytia assay

A syncytia assay was performed to determine the effect of ZnOT on multinucleated cell formation as previously described

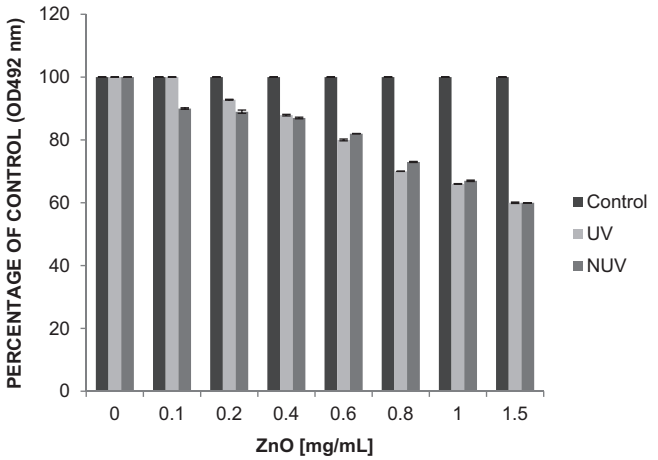

Fig. 1. ZnOT cytotoxicity. The viability of HeLa cells after ZnOT treatment was determined by MTS cytotoxicity assay at 24 h post ZnO treatment. HeLa cells were seeded at a density of 2×10^4 in a 96-well plate. UV ZnOT and NUV ZnOT were brought into suspension in PBS at concentrations of 1.5, 1, 0.8, 0.6, 0.4, 0.2, and 0.1 mg/mL. Cell viability was analyzed by a chromogenic kit (CellTiter Aqueous96; Promega, Madison, WI, USA). Colorimetric detection was measured by micro-pate reader (TECAN GENious Pro) at 492 nm. Results are representative of three independent experiments.

(O'Donnell and Shukla, 2009). Briefly, two populations of cells were generated, target cells and effector cells. Target cell population were transfected with 1.0 μg of gD receptor, nectin-1 and 0.5 μg of a plasmid expressing cyan fluorescent protein (CFP) fused with a nuclear localization signal (NLS) (Clontech, Mountain View, CA). The effector cell population was transfected with 0.5 μg each of HSV-2 glycoproteins gB, gD, gH, and gL and a red fluorescent protein (RFP) fused with a nuclear export signal (NES) (Hu et al., 2003). Target and effected cells were co-cultured in 35 mm glass-bottom dishes (MatTek Corporation) at a 1:1 ratio and treated with 0.1 mg/ml of UV and NUV ZnOT's. Syncytia number and images were captured 24 h post mixing at 63× objective on a confocal microscope (Lecia DMIRE2) equipped with a camera (Lecia TCSSP2). Effector cells lacking gB were used as a negative control for syncytia formation.

2.10. Statistical analysis

Graph Pad Prism software (version 4.0) was used for statistical analysis of each group. $P < 0.05$ and $P < 0.001$ were considered as the significant differences among mock treated and treated groups.

3. Results

3.1. ZnOT effect on cell cytotoxicity

To determine the effect of UV ZnOT and NUV ZnOT treatment on the viability of HeLa and VK2/E6 cells an MTS cytotoxicity assay was performed. A concentration range from 0.1 to 1.5 mg/mL was examined and the highest ZnOT concentration resulted in up to 40 percent loss of viability after the 24 h treatment (Fig. 1). Viability assays also showed comparable effects on by both UV and NUV ZnOT. The concentration of ZnOT during the remainder of experiments was kept at a nontoxic concentration of 0.1 mg/ml throughout the study to preserve cell health during our investigation.

3.2. Neutralization, prophylactic, or therapeutic treatment reduces HSV-2 entry into naturally susceptible cells

Because of the hexagonal wurtzite crystal structure and c-axis as the easy growth axis, one dimensional rods and tetrapods are the most favorable ZnO shapes to grow. In general, growth of various geometries of ZnO nano-microstructures have been performed but there has always been some substrate limitations. The biggest

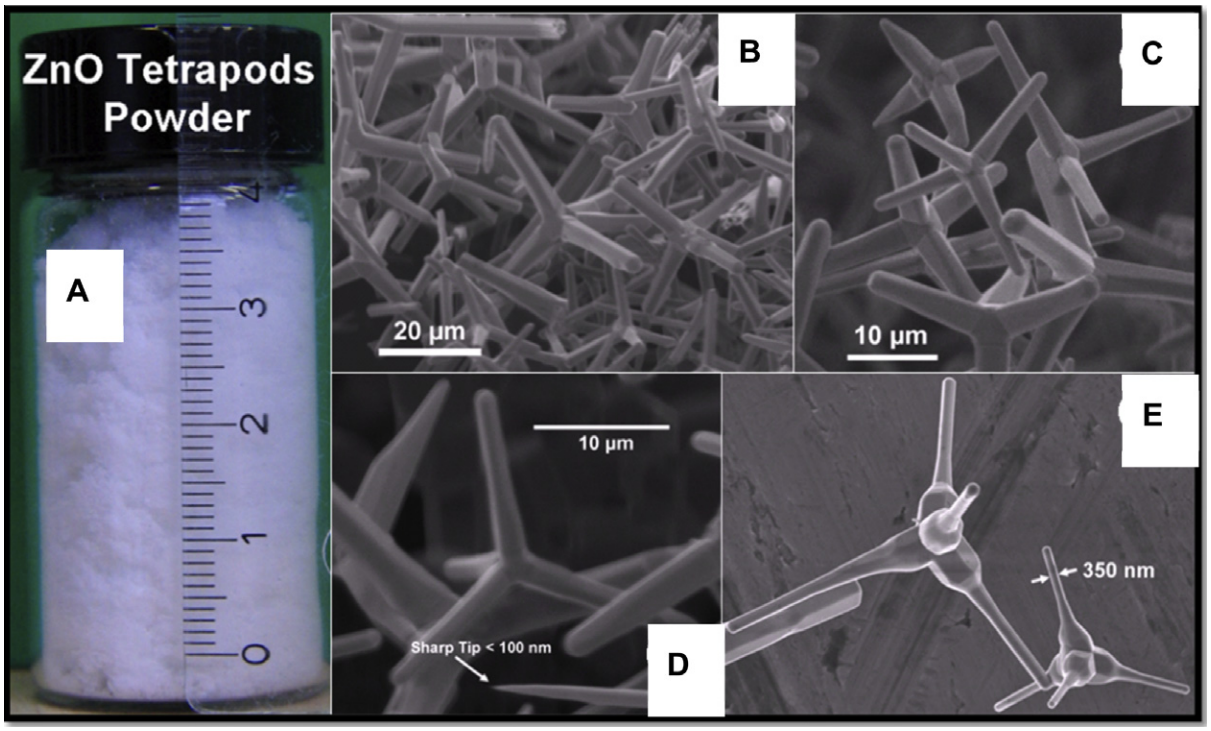

Fig. 2. Zinc oxide nano-micro scale tetrapod structures synthesized by flame transport approach: (A) Glass bottle shows the large amount of ZnO tetrapod structures which were synthesized in just one run. (B–E) show the scanning electron microscopy images of different type of tetrapod structures from the ZnO powder shown in (A).

advantage with flame synthesized ZnO tetrapod structures in the present case is their flexibility that they can be easily used for any application with high accuracy and also there is no substrate limitation (Adelung et al., 2011; Mecklenurg et al. (2012)). For present investigations, large amount of ZnOT were synthesized by already mentioned flame transport approach and correspond SEM images at different magnifications are shown in Fig. 2. SEM images show the tetrapod morphologies and homogeneity of synthesized structures. The diameters of tetrapod arms vary in the range from 200 nm to 2 μm and their lengths vary from 5 to 25 μm which have been successfully reproduced several times as per requirements.

To establish the multifunctional usage of ZnOT structures during different stages of infection, HeLa and V2 K/E6 cells were infected at a concentration of 0.1 mg/ml under three different conditions: neutralization, prophylactic and therapeutic treatment. Each group was contained with UV ZnOTs and NUV ZnOTs. Since UV treated ZnO structures have been reported to show the enhanced antiviral properties (Wiesenthal et al., 2011) thus both UV and NUV ZnOTs were examined to determine their antiviral properties against HSV-2. Following either neutralization treatment in which the virus and ZnOTs were incubated first; prophylaxis treatment (pretreatment of cells with ZnOTs prior to infection), therapeutic treatment (viral infection prior to the addition of ZnOTs), or mock treatment (infection in the absence of ZnOTs), entry of a β-galactosidase-expressing reporter virus, HSV-2(333)gJ−, was determined. As shown in Fig. 3A, the neutralization treatment resulted in a significant decrease ($P < 0.05$) in β-galactosidase expression in HeLa cells and vaginal epithelial cells (data not shown) when treated with both UV and NUV ZnOTs. UV neutralization however resulted in more pronounced decrease of β-galactosidase expression. The prophylactic treatment (Fig. 3B) effect on reporter virus strain HSV-2(333)gJ−, also resulted in a significant decrease in HSV-2 entry in UV ZnOT treated cells ($P < 0.05$) suggesting an enhanced effect of the UV treated ZnOT on the virus. Lastly, the effectiveness of ZnOT in the presence of an active infection was studied through the therapeutic treatment. This condition allowed us to study the inhibiting effects of ZnOTs after viral entry. It has already been shown that HSV is able to enter the cells within the first 10 min of infection at 37 °C (Cheshenko et al., 2003), therefore we allowed the infection to persist for 30 min prior to the addition ZnOTs. Therapeutic treatment with ZnOTs resulted in a decrease in viral entry as expression of β-galactosidase was reduced in UV and NUV ZnOT treated cells, though entry reduction was not as significant as seen in other treatment groups. Treatments were also performed in susceptible VK2/E6 cells (data not shown). A reduction in entry following neutralization, prophylactic and therapeutic treatment was seen in VK2/E6 cells.

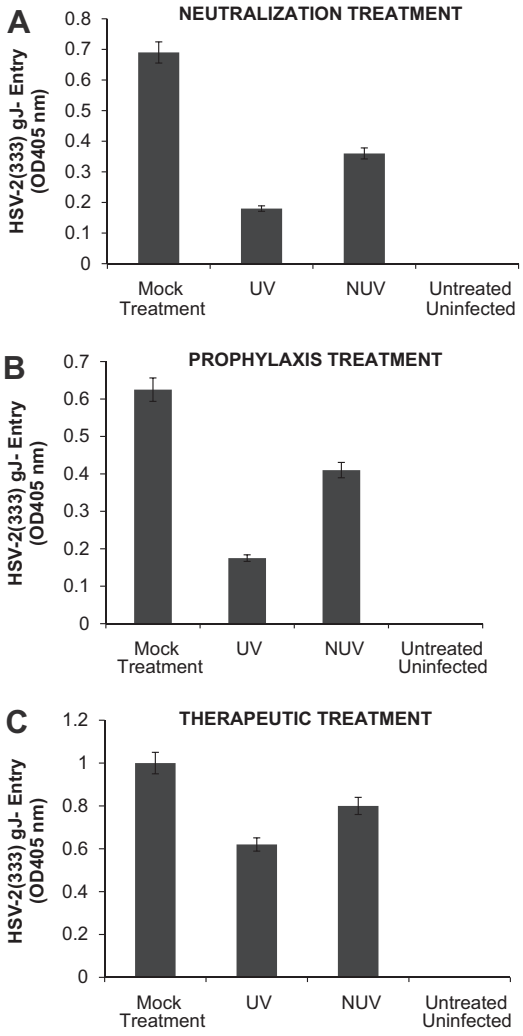

Fig. 3. Neutralization, prophylaxis, or therapeutic treatment with ZnOT inhibits HSV-2 entry. A β-galactosidase-expressing reporter virus, HSV-2(333)gJ was used for entry measurements. Viral entry was determined after each of the treatments indicated. UV treated (UV) or non-UV treated (NUV) ZnOTs were tested. (A) Neutralization. ZnOT was allowed to bind the virus and the virus/ZnOT mixture was then used to infect cells. (B) Prophylaxis treatment. Cells were pretreated with ZnOTs and then infected with HSV- 2(333)gJ− virus. (C) Therapeutic treatment. Cells were first infected with HSV-2(333)gJ− and then treated with the ZnOTs.

3.3. ZnOTs neutralization, prophylaxis and therapeutic treatment decreases internalization of HSV-2(333)

After HSV-2 entry into the cell, VP16 is released from the virion to activate the transcription of immediate early genes. Since VP16 can be immediately detected in cells, it also provides an alternative mechanism to verify HSV internalization. Therefore, to confirm our results obtained using a reporter virus, which could be subjective to the enzymatic activity of the substrate and the translation of the reporter gene, we also focused on detecting VP16 by Western blot analysis. Two hours post infection HeLa cells were collected and total lysates were analyzed to determine the effects of ZnOT on the internalization of VP16. Cells were subjected to neutralization, prophylaxis, or therapeutic treatment. VP16 expression was significantly ($P < 0.001$) decreased following neutralization, prophylaxis, and therapeutic treatment. Under neutralization condition, the effect of UV ZnOTs was most effective in reducing the internalization of the viruses. The oxygen vacancies produced during the UV treatment increases the attraction between ZnOT and the viruses, thus enhancing the viral trapping ability of UV ZnOT in comparison to NUV ZnOT (Fig. 4A). The prophylaxis treatment also resulted in a comparable decrease in HSV-2 (333) internalization in both UV and NUV ZnOTs conditions (Fig. 4B). The decreased internalization, however, supports the preventative function of ZnOT against the ability of viruses to enter into susceptible cells. Lastly, the therapeutical usage of ZnOTs was found to decrease the viral internalization as tegument protein VP16 expression was significantly decreased following UV and NUV ZnOT treatments (Fig. 4C).

3.4. ZnOT treatment inhibits cell-to-cell fusion

One mechanism that has contributed to the pathogenesis of HSV-2 is its ability to infect the neighboring cells without diffusing through the extracellular environment; this is known as cell-to-cell

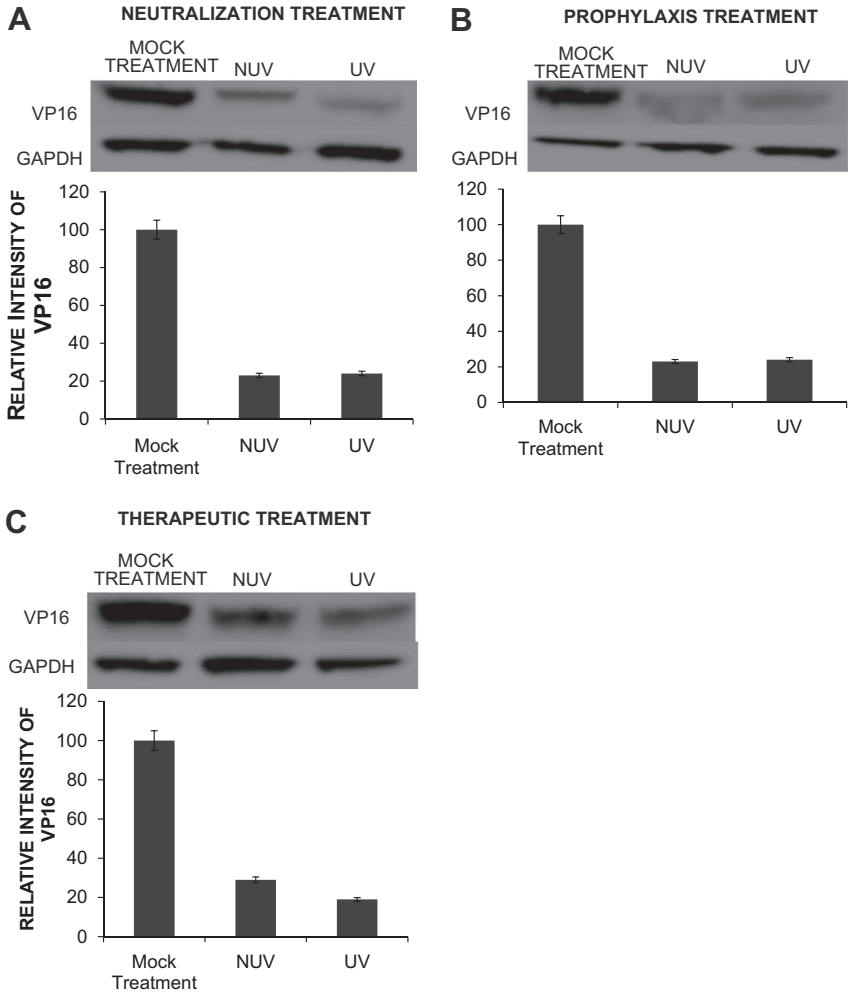

Fig. 4. Neutralization, prophylaxis or therapeutic treatment result in decreased internalization of HSV-2(333). Western blot analysis of VP16 expression was performed to determine the effect of ZnOT on HSV-2 internalization. As indicated, VP16 protein expression was determined for neutralization, prophylaxis, therapeutic or mock treated cells infected with wild-type HSV-2(333). The cell lysates were prepared at 2 h post infection and Western blots were performed. VP 16 expression and relative protein intensity are shown. (A) Neutralization (B) prophylactic and (C) therapeutic treatment. GAPDH was measured as a loading control. Results are representative of three independent experiments.

fusion. Through this process the virus spreads rapidly while evading detection by the immune system (Fischer et al., 2001; Sattentau, 2008). The cell-to-cell spread of viruses is mediated through the coordinated efforts of surface exposed glycoproteins from infected cells that contact their specific receptors on neighboring uninfected cells. Through the specific glycoprotein-receptor interactions, the cells fuse and generate multinucleated cells. Since ZnOTs treatment resulted in a decreased viral entry and internalization, we decided to investigate its effect on virus free cell-to-cell fusion. To create this scenario in vitro CHO-K1 cells were split into two populations: target cells, and effector cells (Tiwari et al., 2009). Target cells were transfected with the gD receptor nectin-1 and the luciferase reporter gene under the control of the T7 promoter. Effector cells were transfected HSV-2 glycoproteins essential for cell fusion and T7 polymerase (Fig. 5A). The fusion between both populations of cells allows the T7-polymerase to bind its promoter thus initiating the synthesis of the luciferase gene. By addition of the substrate, firefly luciferase, we can analyze the amount of fusion that has occurred between the two populations of cells.

To determine the effect of ZnOT treatment on cell-to-cell fusion luciferase activity was measured 18 h post treatment. Effector cells lacking gB mixed with target cells were utilized as a negative control. ZnOT UV and NUV treatment at 0.1 mg/ml resulted in a significant decrease ($P < 0.001$) in the cell-to-cell fusion in CHO-K1 (Fig. 5B). While both forms of ZnOT treatment decreased the cell fusion, UV ZnOT exhibited a larger effect on the fusion of cells than NUV ZnOT. These results illustrate the functional usage of ZnOT's not only at the point of cell entry and viral internalization, but also at the point of viral spread as ZnOTs presence blocks membrane fusion between cells.

3.5. ZnOT treatment decreases infectious cluster size and plaque formation

Since the results of our virus free cell-to-cell fusion assay are subjective to the expression of the luciferase reporter gene, effect of ZnOTs on cell-to-cell spread was assayed in cell culture via an infectious viral spread assay and a plaque assay. The effect of neutralization, prophylaxis and therapeutic treatments at a concentration of 0.1 mg/ml on infectious cluster size was quite astonishing, as cluster size was significantly decreased ($P < 0.05$) (Fig. 6A). The decreased cluster size seen within each group of UV and NUV treated HeLa cells suggests that ZnOTs presence during virus infection regulates the ability of infected cells to fuse with neighboring cells. Furthermore, treatment with ZnOT not only resulted in decreased cluster size, but also reduced the number of virally infected cell

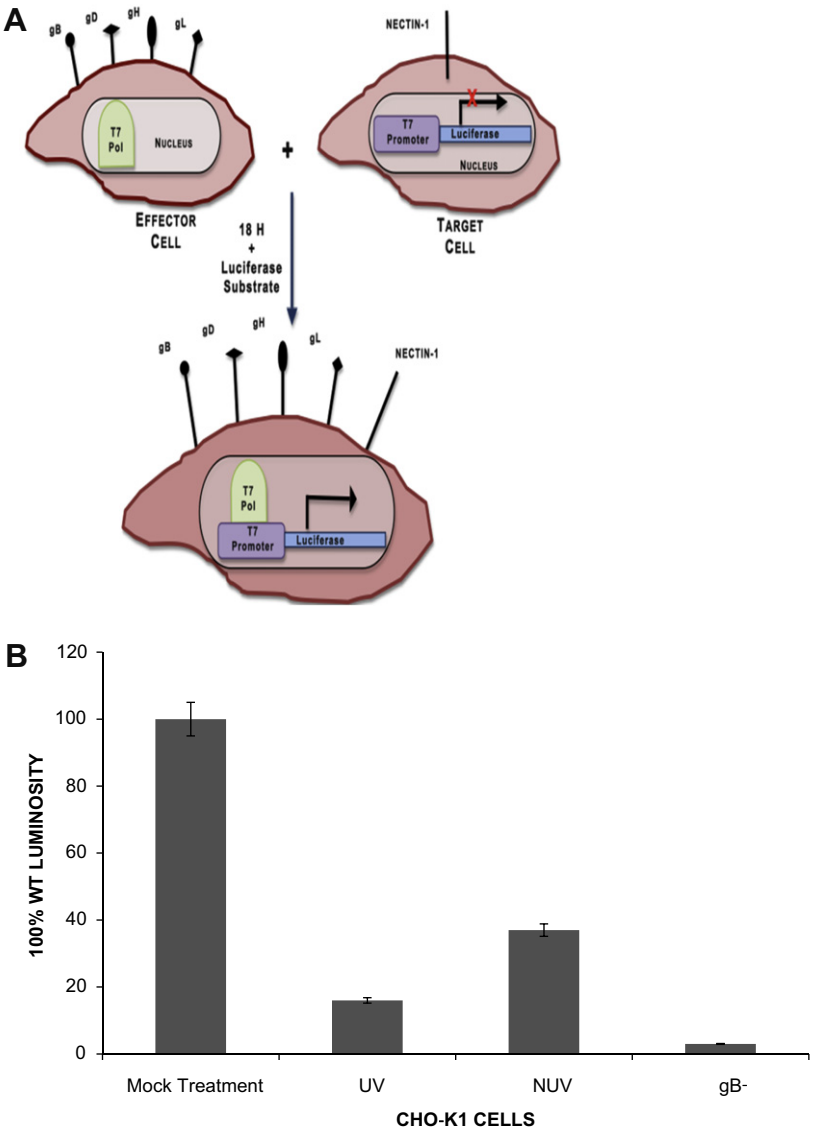

Fig. 5. ZnOT Treatment inhibits virus free cell-to-cell fusion. A. The diagram shows the virus free cell-to-cell fusion assay used. Two populations of cells representing effector cells and target cells were generated. Effector cells express HSV-2 glycoproteins and T7 polymerase and the target cells express gD receptor nectin-1 and the firefly luciferase gene under T7 promoter. The luciferase activity can be detected when the cells fuse. (B) CHO-K1 effector cells were pretreated with UV and NUV ZnOT and mixed with target cells for 24 h. As a negative control effector cells lacking gB were mixed with target cells. Results are representative of three independent experiments.

clusters (Table 1). Under all three ZnOTs treatment conditions, a significant ($P < 0.05$) reduction in infected cell cluster size was observed implying that the lateral diffusion the virus uses during infection is somehow impaired in the presence of both UV and NUV treated cells (Fig. 6B). The significant reduction in infected cell clusters shows that the ZnOT traps virally infected cells thereby decreasing infected cells ability to spread to neighboring cells and disseminate infection.

A viral plaque assay was performed to confirm the results of the infectious cluster assay. Prior to the addition of methylcellulose, an inhibitor of viral diffusion, cells underwent neutralization, prophylaxis, therapeutic, or mock treatment. A stock solution of 0.1 mg/ml was used to treat cells. The ability of HeLa cells to form plaques was almost completely obliterated within each group, supporting the findings of our infectious spread assay. As shown in Fig. 7A, plaque formation and plaque size in the presence of both UV and NUV ZnOTs was dramatically decreased (Fig. 7B). These results were quite impressive as it supports the multifunctional properties of ZnOT at multiple stages of infection and under varying conditions of infection. Following the fixation of cells the number of plaque within each group were counted, and as per our expectation, in the presence of UV and NUV ZnOTs the number of plaques were almost half of that in mock treated cells (Table 2). This suggests that inhibition of the virus infection by ZnOTs prevented both entry and spread of the virus. The statistical significance of the decreased plaque formation within each group supported our prior finding of the inhibitory effect that ZnOT has on viral spread and infection cluster size. Taken together, our results indicate that ZnO tetrapod structures block infection and spread of HSV-2. The significant decrease in plaque number and plaque size suggest that in the presence of ZnOTs, cell susceptibility to infection declines.

3.6. ZnOTs treatment of effector cells reduces syncytial cell formation and reduces the average number of nuclei per syncytia

After entry occurs, the virus is able to spread throughout the host by cell-to- cell fusion. During this process, HSV infected cells express the viral envelope glycoproteins required for fusion on

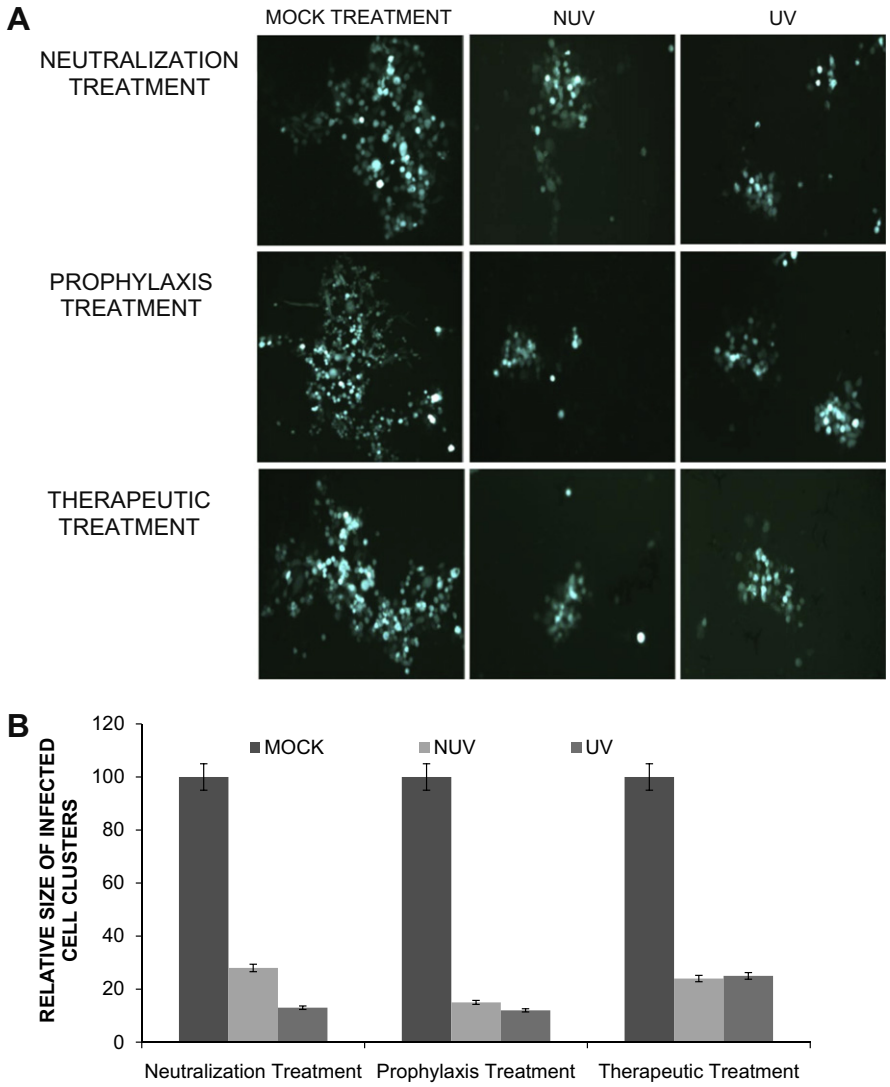

Fig. 6. ZnOT reduces infectious cell cluster formation. HSV-2(333)GFP virus was used to determine the effect of ZnOT on viral replication and cell-to-cell spread. (A) Cellular expression of GFP and its distribution mark the ability of HSV-2 to form clusters of infected cells under various treatment conditions as indicated. Reduced clusters were noted in all conditions where ZnOT was present. (B) Relative sizes of infected cell cultures were determined by measurement of clusters under a fluorescent microscope. Images are representative of 3 independent experiments.

Table 1
Relative number of plaques formed upon ZnOT treatment. The number of plaques was counted after UV ZnOT and NUV ZnOT treatment. Positive control cells were mock treated with 1× PBS. The average is based on the results of three independent experiments.

Relative number of plaques	Mock treatment	NUV treatment	UV treatment
Neutralization treatment	49 ± 8	19 ± 7	17 ± 4
Prophylaxis treatment	61 ± 4	27 ± 5	20 ± 8
Therapeutic treatment	51 ± 3	21 ± 7	12 ± 5

their surface, allowing the infected cell to bind and fuse with neighboring uninfected cells. This results in the formation of large multinucleated cells called syncytia (O'Donnell and Shukla, 2008). To determine the effect of NUV and UV ZnOTs treatment on syncytial formation and number, CHO-K1 cells were split into two populations of cells. The target cells were transfected with a CFP plasmid attached to a nuclear localization signal allowing all transfected cells to have cyan colored nuclei. The effector cells were transfected with a RFP plasmid attached to a nuclear export signal causing all transfected cells to have red cytoplasm (Fig. 8A). The effect of UV and NUV ZnOT treatment significantly decreased the syncytial formation of CHO-K1 cells (Fig. 8B). Table 2 lists the average number of syncytial cells and the size of syncytia in the presence and absence of ZnOT. The results show that cells treated with ZnOT's showed a significant reduction ($P < 0.05$) in their ability to form multinucleated cells (57 syncytial cells) in comparison to positive control cells (99 syncytial cells). The effect of ZnOT treatment was most apparent in cells with >6 nuclei. The effect of ZnOT treatment significantly impaired the size (8 large syncytial cells) in comparison to positive control (22 large syncytial cells). Overall, syncytia formation was reduced to almost half of the number seen in mock treated cells.

3.7. ZnO tetrapod's attraction to HSV-2(333) GFP virus immobilizes virus as virions become trapped in tetrapod spikes

It has been shown that ZnO has the ability to bind and trap HSV-1 (Mishra et al., 2011). This trapping process has been noted to be

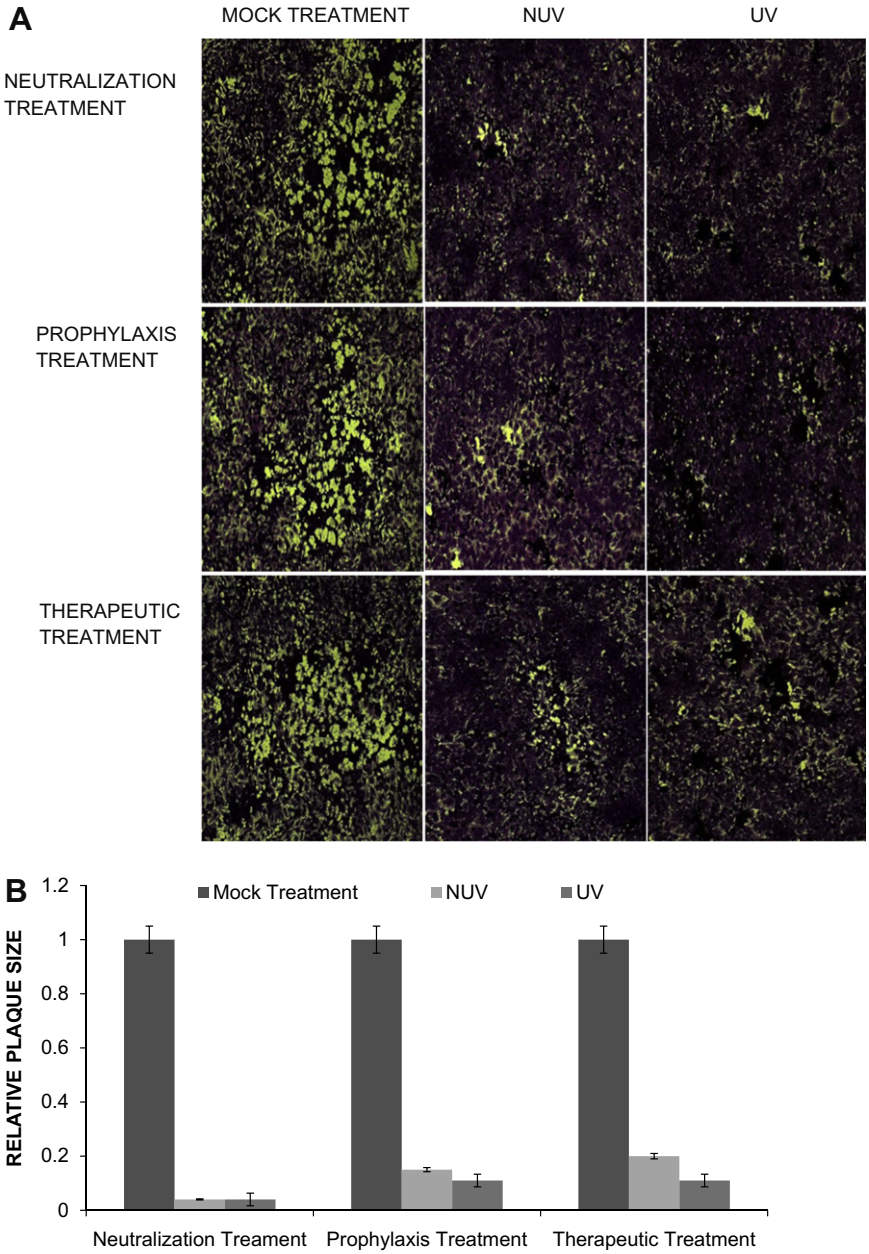

Fig. 7. ZnOT reduces plaque formation. The effect of ZnOT treatment on viral spread and replication was determined by syncytial plaque assay. (A) Formation of plaques by HSV-2(333) infected cells under various treatment conditions as indicated. (B) Relative plaque sizes are shown. The data represents observations from three independent experiments.

Table 2
ZnOT treatment reduces syncytia formation. The average number of syncytical cells and the average number of nuclei per syncytia were counted in CHO-K1 cells after ZnOT treatment. Mock treated target and effector cells were used as a positive control. Target cells lacking gB were mixed with effector cells and used as a negative control. Numbers are an average of 3 independent experiments.

Cell type	Condition	Average syncytia per well	2–3 Nuclei per syncytia	4–5 Nuclei per syncytia	>6 Nuclei per syncytia
CHO-K1	Negative control	0	0	0	0
	Positive control	99	50	27	22
	ZnOT treatment	57	32	17	8

one of the mechanisms in which the nanoparticles neutralizes the virus, thus inhibiting its pathogenesis (Mishra et al., 2011). To determine the interactions between HSV-2 and ZnOT (UV and NUV) were fluorescently stained with phallodin (red) to visualize tetrapod-virus interactions (Fig. 9). Following the staining process tetrapods were incubated with HSV-2(333) GFP to observe the trapping properties of ZnOT to the virus. The confocal microscopy results revealed that both UV and NUV ZnOTs were capable of binding virus. The co-localization of the virus on tetrapod structures suggest that these viruses are attracted to and bind by the ZnOT, therefore making the virus unable to initiate infection within cells.

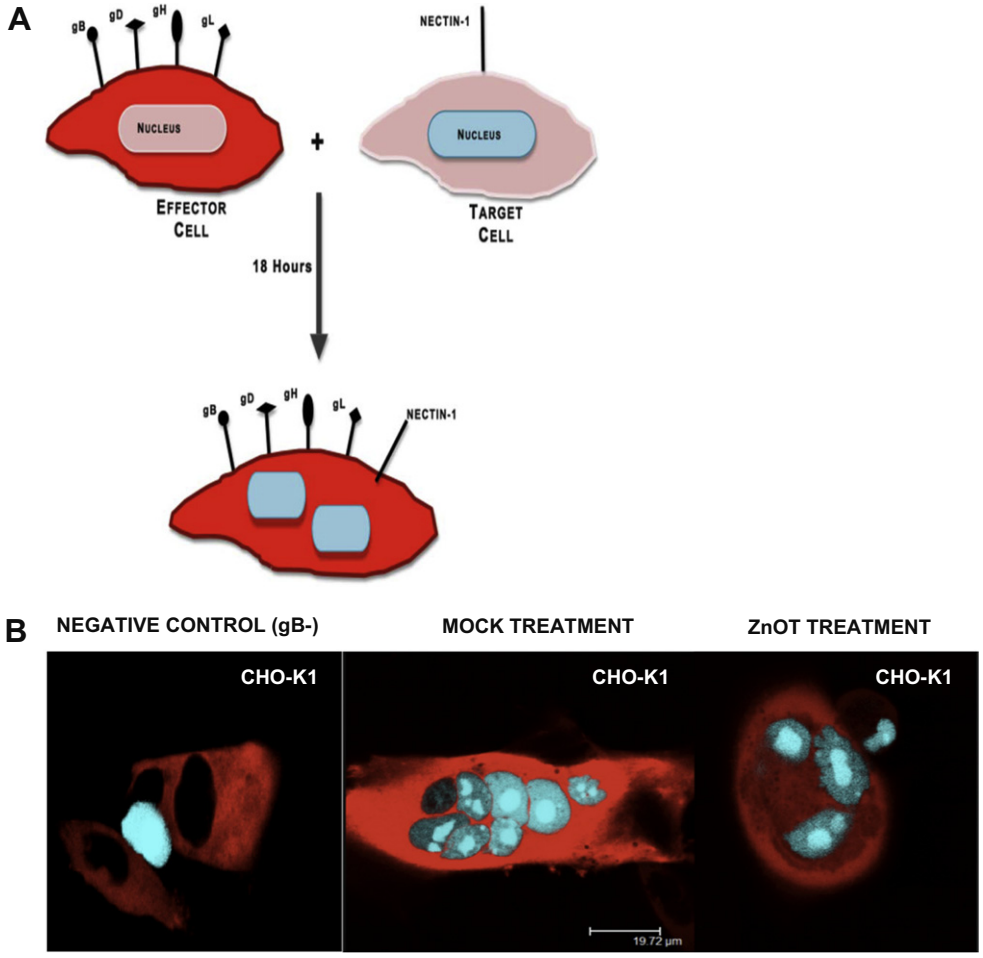

Fig. 8. An illustration of red-blue syncytia assay used to understand the effect of ZnOT treatment. Effector cells expressing HSV-2 glycoproteins required for entry and NES-RFP signal were mixed with target cells expressing gD receptor nectin-1 and CFP-NLS signal. Effectors were pretreated with ZnOT prior to the mixing of target and effector cells. (B) Using a confocal microscope syncytia formation was recorded 24hours post mixing.

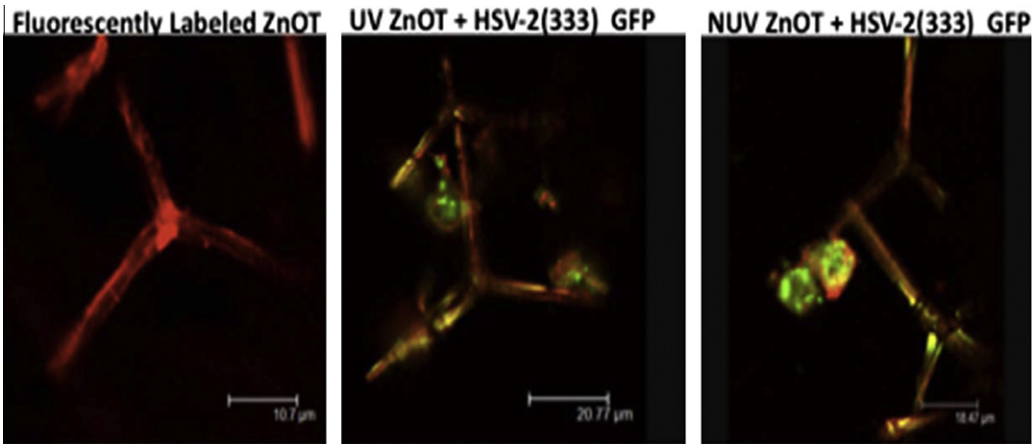

Fig. 9. Fluorescently labeled ZnOT binds HSV-2(333)GFP virus. The direct interactions between ZnOT and HSV-2 virus were visualized through the incubation of fluorescently tagged ZnOT with GFP tagged HSV-2. Both the UV and NUV treated ZnOT show significant trapping ability. Images are representative of 2 independent experiments.

4. Discussion

ZnOT structures utilized in our studies were synthesized by a recently developed flame transport approach (Adelung et al., 2011). This is a very cost effective and efficient approach offering the synthesis of large quantities (>kilograms) of ZnOTs with a high degree of reproducibility. Since these tetrapods are structurally self-supported, they find a wide range of applications ranging from antiviral activities Mecklenurg et al. (2012) to the design of three-dimensional networks as templates for growing multifunctional composite structures (Martinez and Spear, 2002).

This study demonstrates the significance of ZnO tetrapod structures in anti-HSV-2 prevention and therapy. The concept of mounting spikes with diameters down to the nanoscale on a central base

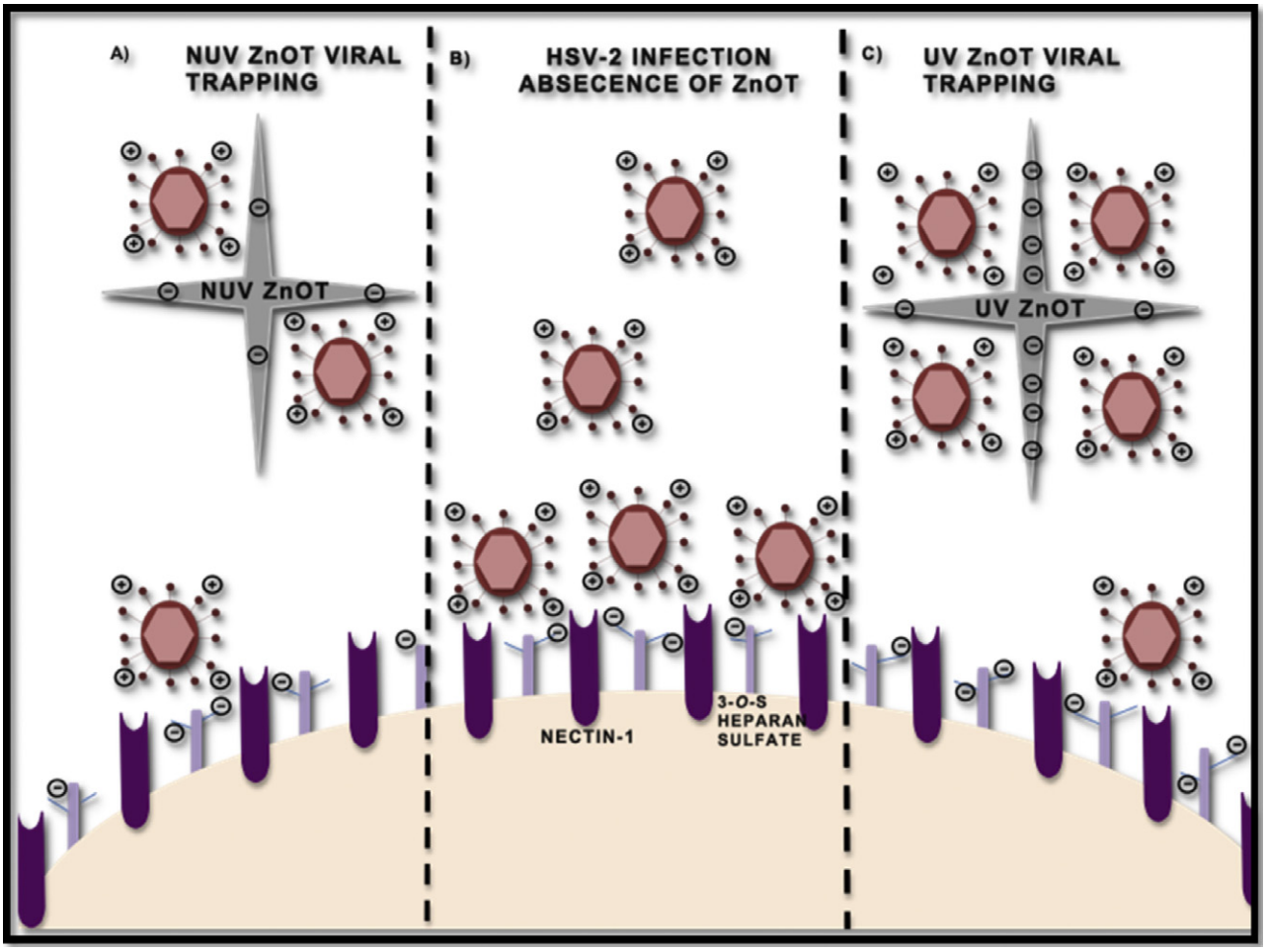

Fig. 10. Model of ZnOT anti-HSV-2 action. A cartoon illustrates the infection process in the presence and the absence of ZnOT. (A) Non-UV treated ZnOT can trap the virus owing to the partial negative charge generated during synthesis. This partial negative charge attracts virus thus contributing to decreased entry and replication. (B) In the absence of ZnOT the virus is able to bind and interact with heparan sulfate and nectin-1 to mediate infection. (C) UV light treatment induces additional oxygen vacancies making ZnOT more partially negative.

creates a micro scale unit that maintains its nanoscale specific functionality. These particles can be seen as nanostructured micro materials. The purpose of this study was to explore the antiviral properties of ZnO micro-nanostructures against HSV-2. The dramatic decrease in infectivity was seen in all experiments whether cells had undergone UV or NUV ZnOT treatments. The consistency of the results shows the promise of ZnOT as a potent anti-HSV agent and also raises the possibility of future development of ZnOT as a broad-spectrum treatment against many viral diseases. Historically, ZnO pastes and powders (Wiesenthal et al., 2011) have been used to treat minor skin irritations such as diaper rashes, eczema, and sunburn (Mishra et al., 2011). Also, the creams that contain zinc oxide and zinc sulfate have been found to reduce symptoms originating from herpes labialis. However, such results were only found upon immediate usage of the creams, and only small favorable differences were seen (Ostelten et al., 2008). An earlier clinical study using ZnO/glycine also showed detectable therapeutic effects among the patients infected with HSV-1 (Godfrey et al., 2001). Thus, the previously performed studies on ZnO also support our findings that our ZnOTs can exert anti-HSV effects and that ZnOTs can be pursued further for development as an alternative treatment to commercially available antivirals.

From a mechanistic view point our study clearly demonstrated the viral trapping ability of ZnO tetrapod structures against HSV-2. Fig. 10 depicts our understanding of the interactions of ZnOTs with HSV-2 preceding a viral infection. The effectiveness of this treatment was not just limited to preventing entry, but it also provided significant therapeutic efficacy by reducing the number of plaques formed after the treatment. The decreased reporter virus expression and production of β-galactosidase signified that treatment with the ZnOT particles resulted in decreased entry. However, since we have utilized a reporter virus system, it was necessary to investigate further if entry was indeed inhibited or the reporter virus expression was altered due to problems with transcription and translation. To rule out any negative effects of reporter virus transcription and translation, we utilized an assay in which results were not dependent on a reporter gene expression but on the direct protein expression of HSV-2 virus. Our investigations led us to determine the effect of ZnOT on the internalization of HSV-2 through detection of the tegument protein VP16. The use of non-toxic concentrations of ZnOT allowed us to conclude that results were solely due to the inhibitory properties of ZnOT in a cell infection system. Once a decrease in internalization was found we also investigated the role ZnOT played in cell-to-cell viral spread and virus-induced membrane fusion. Through both, the viral spread assay and plaque formation assay, we concluded that the presence of both UV and NUV ZnOT inhibited the cell-to-cell spread of HSV-2. These results were later confirmed with the syncytia formation assay and a virus free cell-to-cell fusion assay. We believe that the tetrapod structure and the micro scale dimensions of ZnOTs gener-

ate steric hindrance by specifically binding to HSV-2 infected, and hence, glycoprotein expressing cells and prevent them from fusing with neighboring uninfected cells. This may define a mechanism by which cell-to-cell spread of virus from an infected cell to a neighboring uninfected cell may be inhibited.

Recent exploration of nanoparticle interactions with biological targets has transformed the field of medical research including the area of drug development (Wiesenthal et al., 2011). Nanoparticles now play important roles as biosensors, (Luo et al., 2006) and also provide effective use in drug delivery (De Jong and Borm, 2008). Gold (Au) and Silver (Ag) nanoparticles have been shown to have inhibitory effects on viral infectivity and spread of human immunodeficiency virus type-1 (HIV), respiratory syncytial virus, monkeypox virus, influenza virus, tacaribe virus and hepatitis B Virus (HBV) (Baram-Pinto et al., 2009; Bowman et al., 2008; Galdiero et al., 2011). Silver nanoparticles capped with mercaptoethane (Ag-MES) and gold nanoparticles capped with mercaptoethane sulfonate (Au-MES NP) have been shown as effective inhibitors of HSV-1 infectivity (Baram-Pinto et al., 2010; Baram-Pinto et al., 2009). The high specificity of the Au and Ag nanoparticles to bind HSV-1 particles raises the possibility of developing a new and highly effective microbicide against chronic HSV infections. However, given the high costs associated with Au and Ag, new and cheaper alternatives are highly desirable. In addition nanoparticles could have unforeseen side effects, e.g., it is known that they can overcome the blood brain barrier (BBB) which might not always be intended, furthermore it was recently found that smaller silver nanoparticles could cause inflammation at the BBB (Trickler et al., 2010). An improvement in this respect might be to bind nanostructures to larger units without losing their special features originating from the nanoscale.

Control of the pathogenesis of HSV-2 has been an area of continued interest due to an inability of drugs or vaccines to cure the virus. As the leading sexually transmitted infection, it has a strong global impact on the human health worldwide. While current drugs in the market are used to control the disease symptoms, we are yet to design a prophylactic drug that can be used to prevent transmission of HSV-2. Through our studies we have identified some multifunctional usage of ZnO tetrapod type structures to counteract the infection at different levels. With antiviral resistance increasing against the existing drugs such as acyclovir, the development of board spectrum therapeutics is in great demand, especially those ones which are readily available and can be synthesized at low cost. ZnO micro-nano structures fit both requirements. The mass production of ZnOT structures makes them an ideal product for HSV-2 antiviral therapy. Their ability to control and trap viruses also makes them of specific interest in the development of low cost prophylactics having the potential to treat an existing infections as well. Therefore, we believe that our discovery will indeed have a great impact in the field of therapeutics. While much more groundwork must be done, we believe we are on our way to expanding the list of possible strong candidates for topical treatments for HSV-2 genital lesions. Further in vivo studies in mouse vaginal labia would likely produce insightful information about the antiviral effects of ZnO micro nanostructures in mammalians.

Acknowledgement

This work was supported by National Institutes of Health Grants RO1 AI057860 and AI081869 to D.S. and a core Grant EY01792. D.S. also acknowledges support from Cless Family Foundation. Y.K.M. acknowledges a Grant from AvH foundation; R.A. gratefully acknowledges the funds from DFG from SFB-855 A5, a Heisenberg Professorship, and support from the inflammation at interfaces cluster.

References

Adelung, R., Kaps, S., Mishra, Y.K., Claus, M., Preusse, T., Wolpert, C., 2011. Elastic material with a pore space bridged at the particle level by nanobridges between particles. Patent Pend.: PCT/DE2011/000282, Germany.

Akhtar, J., Shukla, D., 2009. Viral entry mechanisms: cellular and viral mediators of herpes simplex virus entry. The FEBS Journal 276, 7228–7236.

Avitabile, E., Forghieri, C., Campadelli-Fiume, G., 2007. Complexes between herpes simplex virus glycoproteins gD, gB, and gH detected in cells by complementation of split enhanced green fluorescent protein. Journal of Virology 81, 11532–11537.

Baram-Pinto, D., Shukla, S., Gedanken, A., Sarid, R., 2010. Inhibition of HSV-1 attachment, entry, and cell-to-cell spread by functionalized multivalent gold nanoparticles. Small 6, 1044–1050.

Baram-Pinto, D., Shukla, S., Perkas, N., Gedanken, A., Sarid, R., 2009. Inhibition of herpes simplex virus type 1 infection by silver nanoparticles capped with mercaptoethane sulfonate. Bioconjugate Chemistry 20, 1497–1502.

Bowman, M.C., Ballard, T.E., Ackerson, C.J., Feldheim, D.L., Margolis, D.M., Melander, C., 2008. Inhibition of HIV fusion with multivalent gold nanoparticles. Journal of the American Chemical Society 130, 6896–6897.

Campadelli-Fiume, G., Cocchi, F., Menotti, L., Lopez, M., 2000. The novel receptors that mediate the entry of herpes simplex viruses and animal alphaherpesviruses into cells. Reviews in Medical Virology 10, 305–319.

Chayavichitsilp, P., Buckwalter, J.V., Krakowski, A.C., Friedlander, S.F., 2009. Herpes simplex. Pediatrics in Review/American Academy of Pediatrics 30, 119–129; quiz 130.

Cheshenko, N., Del Rosario, B., Woda, C., Marcellino, D., Satlin, L.M., Herold, B.C., 2003. Herpes simplex virus triggers activation of calcium-signaling pathways. The Journal of Cell Biology 163, 283–293.

Connolly, S.A., Jackson, J.O., Jardetzky, T.S., Longnecker, R., 2011. Fusing structure and function: a structural view of the herpesvirus entry machinery. Nature Reviews. Microbiology 9, 369–381.

De Jong, W.H., Borm, P.J., 2008. Drug delivery and nanoparticles:applications and hazards. International Journal of Nanomedicine 3, 133–149.

Favoreel, H.W., Van den Broeke, C., Desplanques, A., Deruelle, M., Van Minnebruggen, G., Nauwynck, H., Glorieux, S., Van Opdenbosch, N., De Regge, N., 2010. Alphaherpesvirus use and misuse of cellular actin and cholesterol. Veterinary Microbiology 143, 2–7.

Fischer, N.O., Mbuy, G.N., Woodruff, R.I., 2001. HSV-2 disrupts gap junctional intercellular communication between mammalian cells in vitro. Journal of Virological Methods 91, 157–166.

Galdiero, S., Falanga, A., Vitiello, M., Cantisani, M., Marra, V., Galdiero, M., 2011. Silver nanoparticles as potential antiviral agents. Molecules 16, 8894–8918.

Godfrey, H.R., Godfrey, N.J., Godfrey, J.C., Riley, D., 2001. A randomized clinical trial on the treatment of oral herpes with topical zinc oxide/glycine. Alternative Therapy in Health & Medicine 7, 49–56.

Hu, C., Ahmed, M., Melia, T.J., Sollner, T.H., Mayer, T., Rothman, J.E., 2003. Fusion of cells by flipped SNAREs. Science 300, 1745–1749.

Jackson, J.O., Longnecker, R., 2010. Reevaluating herpes simplex virus hemifusion. Journal of Virology 84, 11814–11821.

Jin, H., Yan, Z., Ma, Y., Cao, Y., He, B., 2011. A herpesvirus virulence factor inhibits dendritic cell maturation through protein phosphatase 1 and Ikappa B kinase. Journal of Virology 85, 3397–3407.

Kriebs, J.M., 2008. Understanding herpes simplex virus: transmission, diagnosis, and considerations in pregnancy management. Journal of Midwifery & Women's Health 53, 202–208.

Legarra, A., Robert-Granie, C., Manfredi, E., Elsen, J.M., 2008. Performance of genomic selection in mice. Genetics 180, 611–618.

Luo, X., Morrin, A., Killard, A.J., Smyth, M.R., 2006. Application of nanoparticles in electrochemical sensors and biosensors. Electroanalysis 18, 319–326.

Martinez, W.M., Spear, P.G., 2002. Amino acid substitutions in the V domain of nectin-1 (HveC) that impair entry activity for herpes simplex virus types 1 and 2 but not for Pseudorabies virus or bovine herpesvirus 1. Journal of Virology 76, 7255–7262.

Mecklenurg, M., Schuchardt, A., Mishr, Y.K., Kaps, S., Adelung, R., Lotnyk, A., Kienie, L., Schulte, K., 2012. Aerographite: Ultra lightweight flexible nanowall carbon microtube-material with outstanding mechanical performance. Advanced Materials 24, 3486–3490.

Mishra, Y.K., Adelung, R., Rohl, C., Shukla, D., Spors, F., Tiwari, V., 2011. Virostatic potential of micro-nano filopodia-like ZnO structures against herpes simplex virus-1. Antiviral Research 92, 305–312.

Muggeridge, M.I., 2000. Characterization of cell-cell fusion mediated by herpes simplex virus 2 glycoproteins gB, gD, gH and gL in transfected cells. The Journal of General Virology 81, 2017–2027.

O'Donnell, C.D., Shukla, D., 2008. The Importance of heparan sulfate in herpesvirus infection. Virologica Sinica 23, 383–393.

O'Donnell, C.D., Shukla, D., 2009. A novel function of heparan sulfate in the regulation of cell–cell fusion. The Journal of Biological Chemistry 284, 29654–29665.

Ostelten, W., Neven, A., Eekhof, J., 2008. Treatment and prevention of herpes labialis. Canadian Family Physician 54, 1683–1687.

Pertel, P.E., Fridberg, A., Parish, M.L., Spear, P.G., 2001. Cell fusion induced by herpes simplex virus glycoproteins gB, gD, and gH-gL requires a gD receptor but not necessarily heparan sulfate. Virology 279, 313–324.

Roller, R.J., Herold, B.C., 1997. Characterization of a BHK(TK-) cell clone resistant to postattachment entry by herpes simplex virus types 1 and 2. Journal of Virology 71, 5805–5813.

Sattentau, Q., 2008. Avoiding the void: cell-to-cell spread of human viruses. Nature reviews. Microbiology 6, 815–826.
Shukla, D., Liu, J., Blaiklock, P., Shworak, N.W., Bai, X., Esko, J.D., Cohen, G.H., Eisenberg, R.J., Rosenberg, R.D., Spear, P.G., 1999. A novel role for 3-O-sulfated heparan sulfate in herpes simplex virus 1 entry. Cell 99, 13–22.
Shukla, S.Y., Singh, Y.K., Shukla, D., 2009. Role of nectin-1, HVEM, and PILR-alpha in HSV-2 entry into human retinal pigment epithelial cells. Investigative Ophthalmology & Visual Science 50, 2878–2887.
Spear, P.G., 2004. Herpes simplex virus: receptors and ligands for cell entry. Cellular Microbiology 6, 401–410.
Tiwari, V., Clement, C., Duncan, M.B., Chen, J., Liu, J., Shukla, D., 2004. A role for 3-O-sulfated heparan sulfate in cell fusion induced by herpes simplex virus type 1. The Journal of General Virology 85, 805–809.
Tiwari, V., Darmani, N.A., Thrush, G.R., Shukla, D., 2009. An unusual dependence of human herpesvirus-8 glycoproteins-induced cell-to-cell fusion on heparan sulfate. Biochemical and Biophysical Research Communications 390, 382–387.
Trickler, W.J., Lantz, S.M., Murdock, R.C., Schrand, A.M., Robinson, B.L., Newport, G.D., Schlager, J.J., Oldenburg, S.J., Paule, M.G., Slikker Jr., W., Hussain, S.M., Ali, S.F., 2010. Silver nanoparticle induced blood–brain barrier inflammation and increased permeability in primary rat brain microvessel endothelial cells. Toxicological Sciences: An Official Journal of the Society of Toxicology 118, 160–170.
Tronstein, E., Johnston, C., Huang, M.L., Selke, S., Magaret, A., Warren, T., Corey, L., Wald, A., 2011. Genital shedding of herpes simplex virus among symptomatic and asymptomatic persons with HSV-2 infection. The Journal of the American Medical Association 305, 1441–1449.
Wald, A., Langenberg, A.G., Link, K., Izu, A.E., Ashley, R., Warren, T., Tyring, S., Douglas Jr., J.M., Corey, L., 2001. Effect of condoms on reducing the transmission of herpes simplex virus type 2 from men to women. The Journal of the American Medical Association 285, 3100–3106.
Wiesenthal, A., Hunter, L., Wang, S., Wickliffe, J., Wilkerson, M., 2011. Nanoparticles: small and mighty. International Journal of Dermatology 50, 247–254.